

How long range is contour integration in human color vision?*

WILLIAM H.A. BEAUDOT AND KATHY T. MULLEN

McGill Vision Research, Department of Ophthalmology, McGill University, 687 Pine Avenue West, H4-14, Montréal, Canada H3A 1A1

(RECEIVED July 26, 2002; ACCEPTED December 17, 2002)

Abstract

We quantified and compared the effect of element spacing on contour integration between the achromatic (Ach), red–green (RG), and blue–yellow (BY) mechanisms. The task requires the linking of orientation across space to detect a contour in a stimulus composed of randomly oriented Gabor elements (1.5 cpd, $\sigma = 0.17$ deg), measured using a temporal 2AFC method. A contour of ten elements was pasted into a 10×10 cells array, and background elements were randomly positioned within the available cells. The effect of element spacing was investigated by varying the mean interelement distance between two and six times the period of the Gabor elements ($\lambda = 0.66$ deg) while the total number of elements was fixed. Contour detection was measured as a function of its curvature for jagged contours and for closed contours. At all curvatures, we found that performance for chromatic mechanisms declines more steeply with the increase in element separation than does performance for the achromatic mechanism. Averaged critical element separations were 4.6 ± 0.7 , 3.6 ± 0.4 , and 2.9 ± 0.2 deg for Ach, BY, and RG mechanisms, respectively. These results suggest that contour integration by the chromatic mechanisms relies more on short-range interactions in comparison to the achromatic mechanism. In a further experiment, we looked at the combined effect of element size and element separation in contour integration for the Ach mechanism. We found that the critical separation decreases linearly with the spatial frequency, from about 5 deg at low spatial frequency (larger elements) to about 1 deg at high spatial frequency (smaller elements) suggesting a scale invariance in contour integration. In both experiments we also found no differences between closed and open jagged contours detection in terms of element separation. The neuroanatomical implications of these findings relatively to area V1 are discussed.

Keywords: Human color vision, Contour integration, Long-range interactions, Visual cortex, Area V1

Introduction

The contour integration paradigm, relying on the spatial integration of co-oriented and collinear cues across the visual field, has been extensively used to investigate the spatial properties of the linking process involved in contour-based shape perception (Field et al., 1993; Kovacs & Julesz, 1993; McIlhagga & Mullen, 1996; Mullen et al., 2000; see Hess & Field, 1999 for a review). It has been proposed (Field et al., 1993; Kovacs, 1996; Polat, 1999) that this spatial linking is mediated by long-range horizontal connections in the primate striate cortex (V1) that link distant neurons with similar orientation properties and form nonclassical receptive fields (Mitchison & Crick, 1982; Rockland & Lund, 1983; Ts'o & Gilbert, 1988; Malach et al., 1993; Kapadia et al., 1995; Zipser et al., 1996; Sincich & Blasdel, 2001). However, it is not yet known to what extent these long-range connections are limiting

contour integration, and how their facilitatory effect is modulated by chromaticity, spatial frequency, or other visual attributes. Investigating the effect of the interelement distance on contour integration should tell us more about the nature of the long-range interactions involved in this process.

Although there is a wealth of literature on the effect of spacing on line detection in dots grouping (see for example: Uttal, 1987; Zucker & Davis, 1988; Kubovy et al., 1998), no other study has systematically investigated the effect of element separation *per se* on contour integration using Field et al.'s paradigm. Previous studies on contour integration have either investigated the effect of relative densities of contour and background elements on contour saliency (Kovacs & Julesz, 1993; Kovacs et al., 1999; Pennefather et al., 1999), or looked at the effect of curvature, contrast, and chromaticity in dense arrays where no relative density is present between contour and background elements (Field et al., 1993; McIlhagga & Mullen, 1996; Mullen et al., 2000). In the former task, the cue for contour detection is mainly a difference in density, while in the latter contour detection is subserved by orientation continuity, better corresponding to a contour integration task. In particular, Field et al. (1993) have looked at the qualitative effect of element spacing by measuring performance at three element separations (0.25, 0.5, & 0.9 deg corresponding to 2, 4, and 7.2 λ , the wavelength of the elements). They reported that, although

Address correspondence and reprint requests to: William H.A. Beaudot, McGill Vision Research, Department of Ophthalmology, McGill University, 687 Pine Avenue West, H4-14, Canada H3A 1A1. E-mail: william.beaudot@mcgill.ca

*This work was initially reported to the 2001 Meeting of the Association for Research in Vision and Ophthalmology, Fort Lauderdale, Florida, USA (IOVS 42/4, S515).

performance decreases with distance, contour integration can be performed over a wide range of distances, implying interactions over large areas of the visual field and beyond classical receptive fields. Interestingly, it has been demonstrated, using relatively dense element arrays (element separation of 2.5λ), that the blue–yellow (BY), red–green (RG), and achromatic (Ach) mechanisms perform similarly on contour integration (McIlhagga & Mullen, 1996; Mullen et al., 2000), suggesting a common process. On the other hand, we have also found that Gabor arrays of identical physical densities are not perceived equally by the three postreceptoral mechanisms (Beaudot & Mullen, 2000); BY arrays are perceived as significantly more dense than either RG or Ach stimuli.

In this paper, we investigate the effect of element separation on contour integration with three parallel aims. The first aim is to quantify and compare its effects between the three postreceptoral mechanisms, and to this end we perform our experiment with three cardinal stimuli (RG, BY, and Ach). Our second aim is to determine how element separation and contour curvature jointly affect contour integration, and how this follows the co-circularity rule of Parent & Zucker (1989). The third is to determine the combined effect of element size and element separation on contour integration by the Ach mechanism.

Methods

Stimuli

The contour integration paradigm of Field et al. (1993) requires the linking of orientation across space to detect a contour. The stimuli

were square arrays (10×10 elements) of pseudorandomly distributed Gabor elements (Fig. 1A). The subject's task was to detect a "path" (open or closed) which consisted of a set of ten oriented Gabor elements aligned along a common contour, embedded in the background of similar but randomly oriented Gabor elements. Inspection of Fig. 1A reveals that the contour in the example winds horizontally across the figure. Gabor elements were used to limit the spatial bandwidth of the stimuli (Field et al., 1993; McIlhagga & Mullen, 1996; Mullen et al., 2000). The elements were odd symmetric and defined by the equation

$$g(x, y, \theta) = c \sin(2\pi f(x \sin \theta + y \cos \theta)) \exp - \left(\frac{x^2 + y^2}{2\sigma^2} \right), \quad (1)$$

where θ is the element orientation in degrees, (x, y) is the distance in degrees from the element center, and c is the contrast. Following our previous study (Mullen et al., 2000), we used elements of low spatial frequency ($f = 1.5$ cpd) with a space constant of a quarter of the wavelength ($\sigma = 0.17$ deg).

A temporal 2AFC procedure was used to measure the subject's ability to detect the contour by discriminating between the contour stimulus and a no-contour stimulus which consisted only of randomly placed Gabor elements. The no-contour stimulus was constructed with the following algorithm. The stimulus area was divided into a 10×10 grid of equally sized cells. The cell size (cs) was chosen to be compatible with the average distance between neighboring elements defined by the element spacing (es), that is $cs \approx 2es/(1 + \sqrt{2})$. A Gabor element of random orientation was placed in each cell with the restriction that each cell contained the

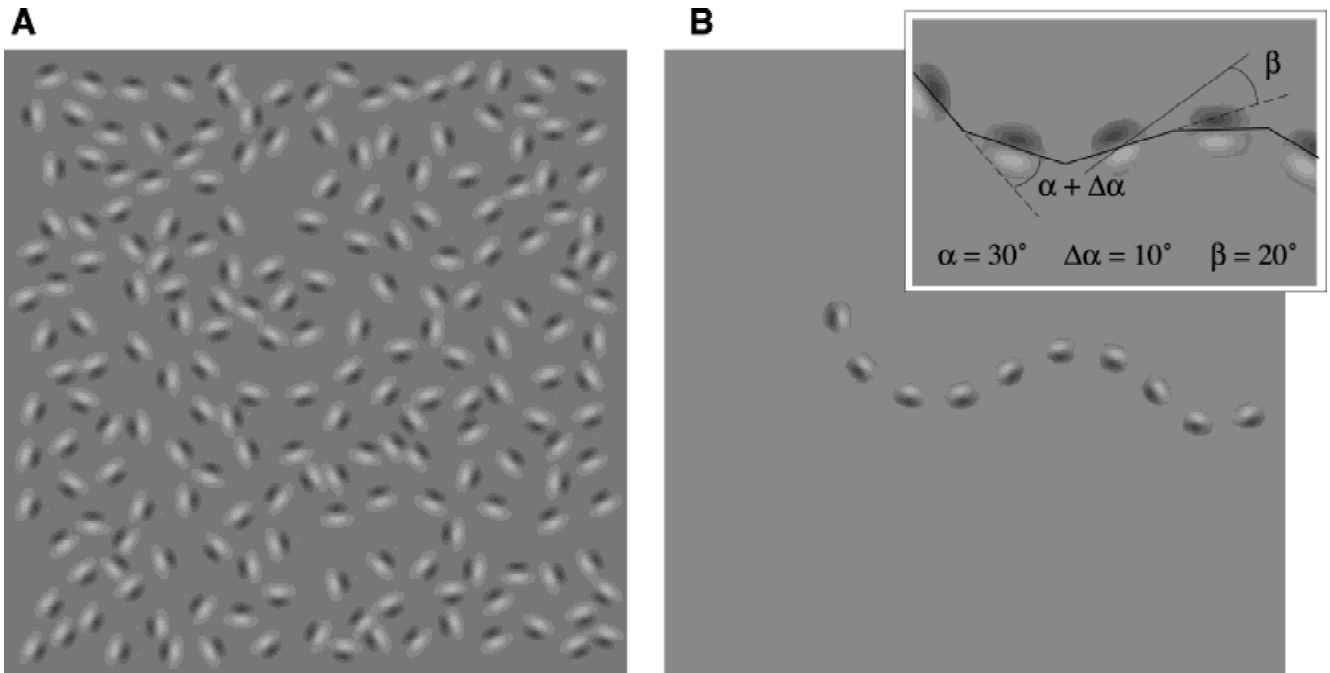


Fig. 1. A: An example of stimulus. The contour is difficult to detect when embedded in a background of similar but randomly oriented elements. Experienced subjects perform typically at around 80% correct under a steady presentation of 500 ms and for a curvature of 20 deg. B: The contour is shown separated from the background elements. It is a chain of ten Gabor elements which vary systematically in their orientation, as described in the inset. *Inset:* The contour is made up of ten backbone line segments. The orientation difference between each successive line segment is given by the angle α which in this case is ± 30 deg. α determines the contour curvature. $\Delta\alpha$ is a small orientation jitter added to α and is uniformly distributed between ± 10 deg. β gives the orientation of the Gabor element with respect to the backbone element. β is zero in experiments presented in this paper. Note that Gabor elements are odd-symmetric and aligned in phase.

center of only one Gabor element. This pseudorandom placement prevents clumping of the elements. Overlap of the elements was also prevented by restricting the placement of their centers within the cell. It was sometimes impossible to place a Gabor element in its cell because it would be too close to elements previously placed. This produced an empty cell, and no more than eight empty cells were permitted in a display and the average number was four.

The contour stimulus can be considered as two parts, the ten elements forming a path and the background elements. A set of path elements is shown in Fig. 1B, and its construction is illustrated in the inset. The path has a “backbone” of ten invisible line segments. The shape of the backbone is controlled by the parameter α (curvature) that determines the angle difference between adjacent backbone elements. Higher values of α produce more curvature in the contour, and lower values produce straighter contours. Two types of paths were generated: open jagged contours (the sign of curvature varies along the path, $\pm\alpha$) and closed contours ($\alpha = 36$ deg for ten elements). To avoid the occurrence of absolutely straight contours when α is 0 deg, an orientation jitter uniformly distributed between ± 10 deg was added to α . The length of each segment was randomly selected so the average distance between the centers of two consecutive segments was the same average distance as between background elements. Gabor elements were placed in the middle of each line segment with the same orientation. Finally, to avoid random closure of the open jagged contours with a high curvature, which can affect detection (Elder & Zucker, 1993; Kovacs & Julesz, 1993), paths that looped back on themselves were discarded and new ones generated. Closed contours were built in the same manner as open jagged contours with an additional constraint: their segment extremities had to form a closed backbone. Closed contours not satisfying this constraint were also discarded. The entire path was pasted into the display at a random location, making sure that the centers of the Gabor elements occupied different cells, and that at least one path element passed through the central region of the stimulus (defined as a circular region 3 deg in diameter), minimizing the search area. In addition to this positional constraint, the use of contours made of ten elements in a 10×10 array has the implicit advantage of constraining the whole contour to be centered on the stimulus. Given that contour integration reaches asymptotic performances for contours of only five to six elements, this configuration reduces the possibility that contour detection is limited by the most peripheral elements (see Hess & Dakin, 1997). Finally, the remaining empty cells were filled with randomly oriented Gabor elements, as in the no-contour stimulus. Various control measurements described previously have demonstrated that no spurious cues could be used for contour detection (Mullen et al., 2000).

Chromatic representation of the stimuli

The chromaticity of the stimuli was defined using a three-dimensional cone contrast space in which each axis represents the quantal catch of the L, M, and S cone types normalized with respect to the background. Stimulus chromaticity and contrast is given by a vector direction and magnitude, respectively, within the cone contrast space. In all experiments only the three cardinal stimuli were used. These are designed to isolate each of the three different postreceptoral mechanisms and have been described previously (Mullen et al., 2000).

Apparatus and calibrations

Stimuli were displayed on a Sony Trinitron monitor (GDM-F500R) driven by a VSG 2/4 graphics board (Cambridge Research Systems Ltd., Rochester, England) with 15-bits contrast resolution, housed in a Pentium PC computer. The frame rate of the display was 76 Hz. The spectral emissions of the red, green, and blue guns of the monitor were calibrated using a PhotoResearch PR-650-PC SpectraScan (Chatsworth, CA). The monitor was gamma corrected in software with lookup tables using luminance measurements obtained from an OptiCAL gamma correction system interface with the VSG display calibration software (Cambridge Research Systems). The Smith and Pokorny fundamentals (Smith & Pokorny, 1975) were used for the spectral absorption of the L, M, and S cones. From these data, a linear transform was calculated to specify the phosphor contrasts required for given cone contrasts (Cole & Hine, 1992). The monitor was viewed in a blacked-out room. The mean luminance of the display was 60 cd/m². The stimuli were viewed at 60 cm. Stimuli were generated on-line, and a new stimulus was generated for each presentation.

Protocol

In each experimental condition, the mean distance between background and contour elements was the same, and the stimuli were carefully designed so no density cue could allow the detection of contour elements. The total number of elements was fixed (10×10) and the element spacing (es) was varied across experimental conditions as a multiple of the wavelength (λ) of the elements ($\lambda = 0.66$ deg, $es = 2-5 \lambda$ in the first experiment; λ and es depend on the spatial frequency in the second experiment). As a consequence, the stimuli subtended 11×11 deg (2λ) to 27×27 deg (5λ) of visual angle (Fig. 2) in the first experiment, and were scaled versions of these in the second experiment (Ach only). In the first experiment, we also included a stimulus condition corresponding to 6 times the wavelength for slightly smaller elements ($f = 1.8$ cpd) to deal with the limitation of the display size.

Contour detection was measured using a temporal 2AFC procedure with a 500-ms interstimulus interval as a function of curvature (0–40 deg) for each postreceptoral mechanism and at a fixed suprathreshold contrast for contour integration (50% for Ach, 12% for RG, and 75% for BY). We have previously shown that contour detection is relatively independent of suprathreshold element contrast (Mullen et al., 2000; Hess et al., 2001). In separate sessions, we measured performance for detecting open and closed contours in stimuli presented for 500 ms. The number of trials per session for each experiment was 50 for each subject, and three to four sessions were performed for each condition on average. Auditory feedback was given after each trial. A black fixation mark was presented briefly at the beginning of each session in the center of the display.

Observers

The observers were two naïve volunteers (JAH & SAL) and the two authors (WB & KTM). All four have normal or refracted-to-normal vision, and all have normal color vision according to the Farnsworth-Munsell 100-Hue Test. All experiments were done under binocular conditions. Naïve subjects had practice trials before the experiments commenced to reach a performance level identical to the two authors.

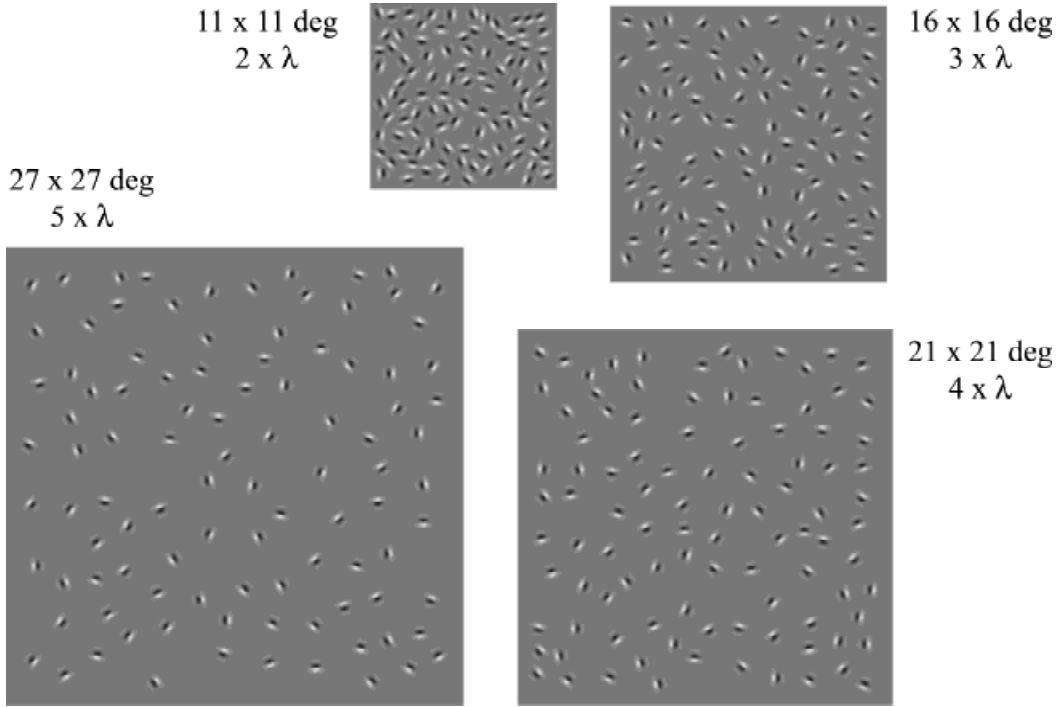


Fig. 2. Examples of contour stimuli used in the first experiment with element spacing varying from two to five times the wavelength of the elements, and with the size ($f = 1.5$ cpd; $\sigma = 0.17$ deg) and number of elements (10×10 elements) remaining the same across all conditions. The size of each cell containing a Gabor element was constrained by the element spacing defining the average distance between neighboring elements. This makes the size of the array vary from about 11×11 deg for a spacing of 2λ to about 27×27 deg for a spacing of 5λ .

Results

Effect of chromaticity

Figs. 3–6 show performance as a function of element separation and curvature for four subjects for detection of open and closed contours, and for each postreceptoral mechanism. As reported previously (Mullen et al., 2000), asymptotic performance decreases with curvature for each mechanism (Fig. 3–5). Performance also generally decreases smoothly with element separation. It is noteworthy that the performance at the lowest separation (2λ) is always better for closed contours (with a curvature of 36 deg) than for open contours of similar curvature (30–40 deg). However, the decrease with element separation is generally more pronounced for closed contours than for open contours. Depending on the subject, the decrease of performance for open contours with element separation appears more pronounced for RG (Fig. 4) and BY (Fig. 5) mechanisms than for the Ach one (Fig. 3). This difference between Ach and chromatic postreceptoral mechanisms is larger for the detection of closed contours (Fig. 6).

To analyze these data, we calculated a critical element separation as a function of curvature by fitting these data with a Weibull function corrected to take the differing asymptotic levels into account:

$$PC(x) = 50 + (pc_{\max} - 50) \times e^{-(x/S)^\beta}, \quad (2)$$

where PC is percent correct, pc_{\max} is the asymptotic performance level, S is the separation threshold, β is the slope, and x is the

element separation. The threshold (S) of this function is $1/e$ % of the asymptotic level relative to guess level, and it was corrected back to $(1 - 1/e)$ % to derive the critical element separation with the formula: $A = S[-\ln(1 - e^{-1})]^{1/\beta}$. In a similar way, we calculated a critical curvature as a function of the element separation. Although the majority of the data sets could be fitted appropriately, some could not be fitted and have not been included in the subsequent analysis. This is due to the fact that we could not always use large enough element separation resulting in a significant drop in performance. The range of element separation is limited by the size of the display and the fixed number of elements.

Fig. 7 shows for all four subjects the critical element separations in wavelength units as a function of curvature for open contours with filled symbols and for closed contours with open symbols. The critical separation, as defined above, characterizes the spacing between elements above which performance for contour detection drops by a criterion amount. First, for all subjects and for the three postreceptoral mechanisms, the critical element separations are almost flat with contour curvature. Second, subjects WB and SAL show a differential effect of the Ach mechanism compared to both chromatic mechanisms: for both open and closed contours, the critical element separation for Ach is about 1.5 times higher than the critical separations for BY and RG. Depending on the stimuli configuration (open or closed) both subjects also show a higher critical separation for BY than for RG (1.5 times for closed contours for WB, and for open contours for SAL). In contrast with these two subjects, the two others (JAH and KTM) show no significant difference in critical element separation be-

Ach Contour detection vs Element separation

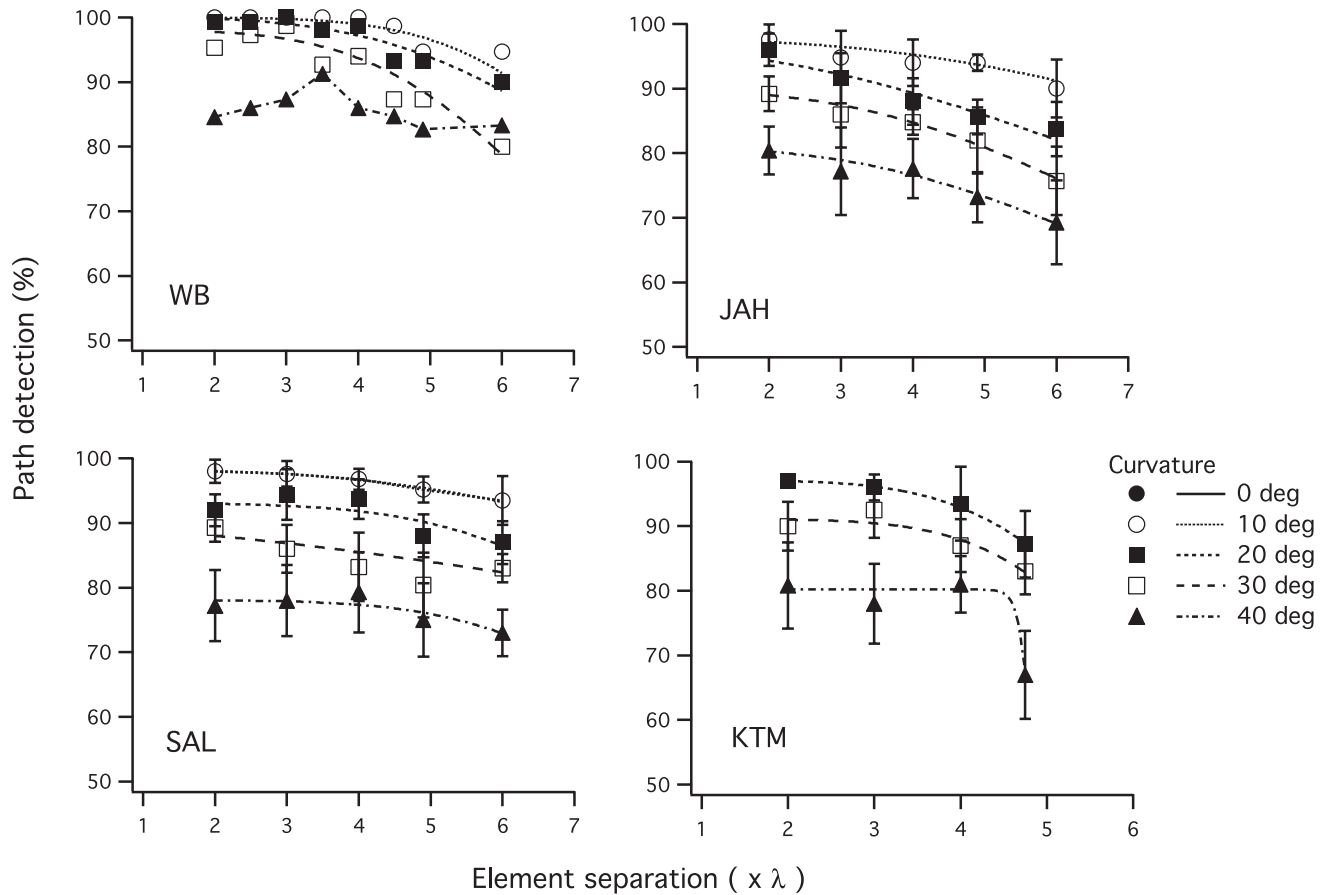


Fig. 3. Performance in jagged contour detection for all four subjects as a function of element separation at different curvatures for the Ach mechanism. Smooth lines represent fits by eqn. (2). Note that one data set for WB could not be fitted. Error bars denote standard deviations.

tween Ach and BY (about 7.3λ for JAH and 5.2λ for KTM). JAH shows a significantly higher critical separation (1.5 times for open contours) for Ach and BY compared to RG, while KTM shows no difference in critical separation between mechanisms. Finally, for all subjects there is no evidence that critical element separation is higher for closed contours than for open contours.

Fig. 8A shows the critical element separation averaged across subjects as a function of curvature for the three postreceptoral mechanisms. For each curvature condition, the critical separation is the highest for the Ach mechanism, and significantly lower for the two chromatic mechanisms, with a slight but constant advantage for BY compared to RG. For the three mechanisms the critical separation is relatively flat with curvature, with no difference between open and closed (curvature condition of 36 deg, as indicated by the arrow) contours. These critical separations are averaged across curvatures in Fig. 8B (closed contour condition included), and are 6.8 ± 1.0 , 5.4 ± 0.6 , and $4.3 \pm 0.3 \lambda$ units for Ach, BY, and RG, respectively. These critical element separations correspond to 4.6 ± 0.7 , 3.6 ± 0.4 , and 2.9 ± 0.2 deg of visual angle for Ach, BY, and RG, respectively. Fig. 8C shows the critical curvature averaged across subjects as a function of element separation for the three postreceptoral mechanisms. For each element separation condition, the critical curvature is the highest for the

Ach mechanism, and significantly lower for the two chromatic mechanisms, with an advantage for BY compared to RG only at the highest element separation. For the three mechanisms the critical curvature is flat with the element separation (except for RG at the higher separation). This is consistent with the relative independence of critical separation on curvature noted above, indicating that curvature and element separation do not interact in contour integration. The critical curvatures are averaged across element separations in Fig. 8D, and are 39.2 ± 1.4 , 32.7 ± 0.9 , and 28.6 ± 4.6 deg for Ach, BY, and RG, respectively.†

†The Ach critical curvature (about 40 deg) is higher than the one we reported in a previous experiment (20–30 deg for an element spacing of 2.5λ , see Fig. 5 p. 646 in Mullen et al., 2000), and reveals a difference between Ach and chromatic mechanisms at suprathreshold contrasts we did not find previously. The only difference in the present experimental setup is a higher mean luminance (60 cd/m^2 vs. 14 cd/m^2) due to the use of a different CRT display. There is no clear explanation for this selective Ach improvement in critical curvature, but it may be linked to the decrease of spatial summation in orientation selectivity at higher background luminance as suggested by Vassilev et al. (1989). This improvement cannot be explained by a relative effect of mean luminance on contrast sensitivity because the contrast sensitivity is expected to be independent of light level in both studies (Rovamo et al., 2001).

RG Contour detection vs Element separation

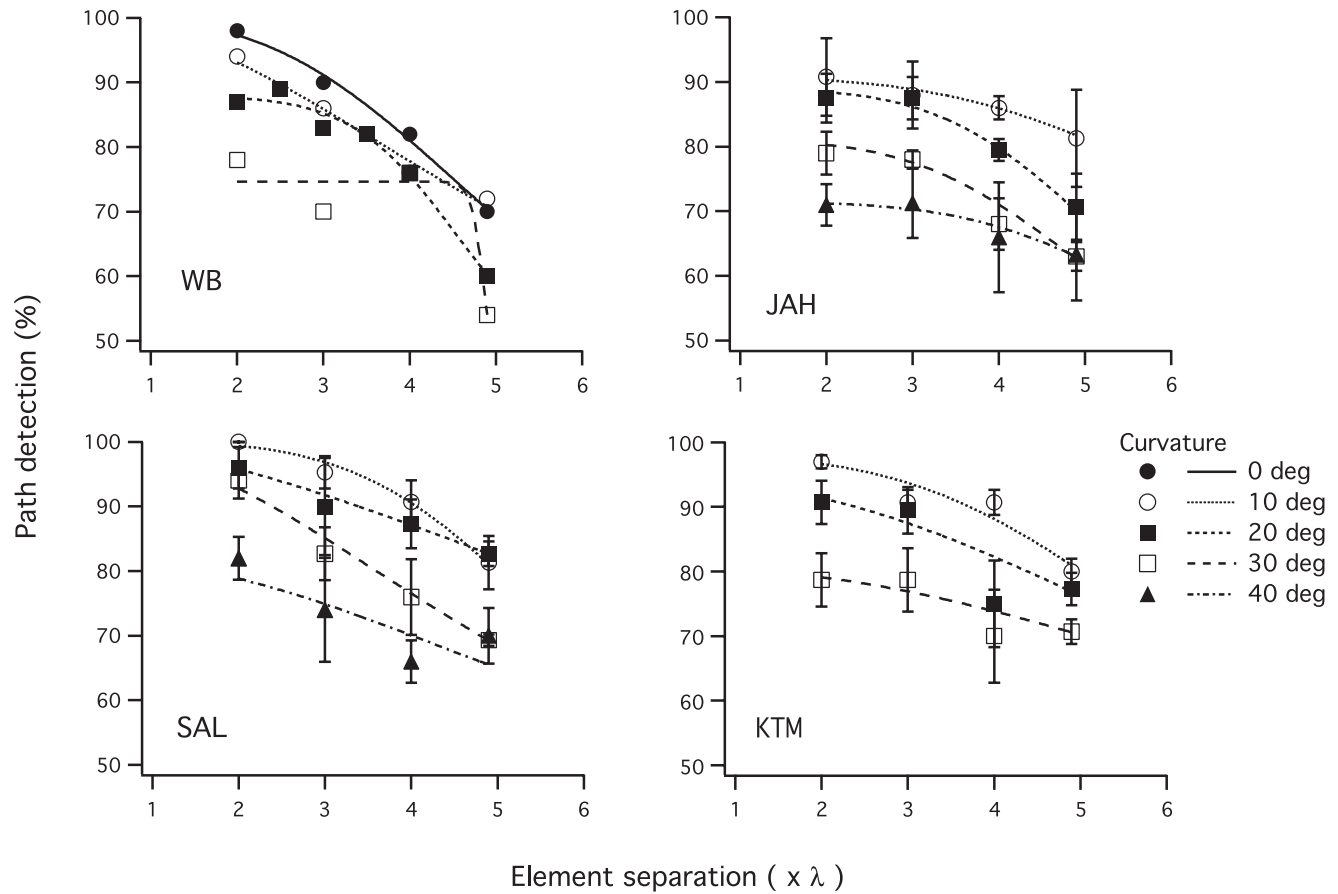


Fig. 4. Performance in jagged contour detection for all four subjects as a function of element separation at different curvatures for the RG mechanism. Smooth lines represent fits by eqn. (2). Error bars denote standard deviations.

Effect of element size

In this experiment, we looked at the combined effect of element separation and spatial frequency of the elements on Ach contour integration. Three subjects (WB, JAH, & SAL) repeated the 2AFC task for open and closed Ach contours. In different sessions, the spatial frequency was varied between 1.5 and 6 cpd (with a space constant $\sigma = \lambda/4$), and the element separation, depending on the element size, was varied between 2 and 15 times the element wavelength. For the open jagged contours, only one curvature was used (20 deg). We analyzed the data similarly to the first experiment; performances for contour detection as a function of element separation for each spatial frequency were fitted with eqn. (2), and a critical element separation was derived for each spatial frequency. Fig. 9 shows the critical separation as a function of spatial frequency for each subject and averaged across subjects (bottom right). In each graph, critical separations are expressed as multiples of the element wavelength (open symbols, left axis) and degrees of visual field (filled symbols, right axis). First, critical separation expressed in multiples of element wavelength is band-pass in spatial frequency for both open and closed contours (except closed contour condition for subject WB) with the highest element sep-

aration (above 10λ) at about 4.5 cpd. There is also no consistent advantage of closed versus open contours. The two naïve subjects show an opposite trend consistent across spatial frequencies, while subject WB shows a constant critical separation for closed contours. Second, critical separation expressed in degrees of visual field is decreasing monotonically with the spatial frequency for all subjects and both open and closed contour conditions. When averaged across subjects, there is no significant difference in element separation between detection of open and closed contours. The averaged critical separation expressed in λ units is still slightly band-pass with spatial frequencies, starting from 7λ at low spatial frequency, up to 12λ at medium frequency, and down to $4\text{--}6 \lambda$ at high spatial frequency. When expressed in degrees of visual field, the averaged critical separation decreases almost linearly with the spatial frequency from 4.6 deg at low spatial frequency to 0.8 deg at high spatial frequency. This result demonstrates that contour integration follows a scale invariance as previously suggested by Hess and Dakin (1997), who reported that contour detection is constant over a wide range of viewing distances. Small elements (of high spatial frequency) are linked over small distances (about 1 deg at 6 cpd), while large elements (of low spatial frequency) are linked over larger distances (about 5 deg at 1.5 cpd).

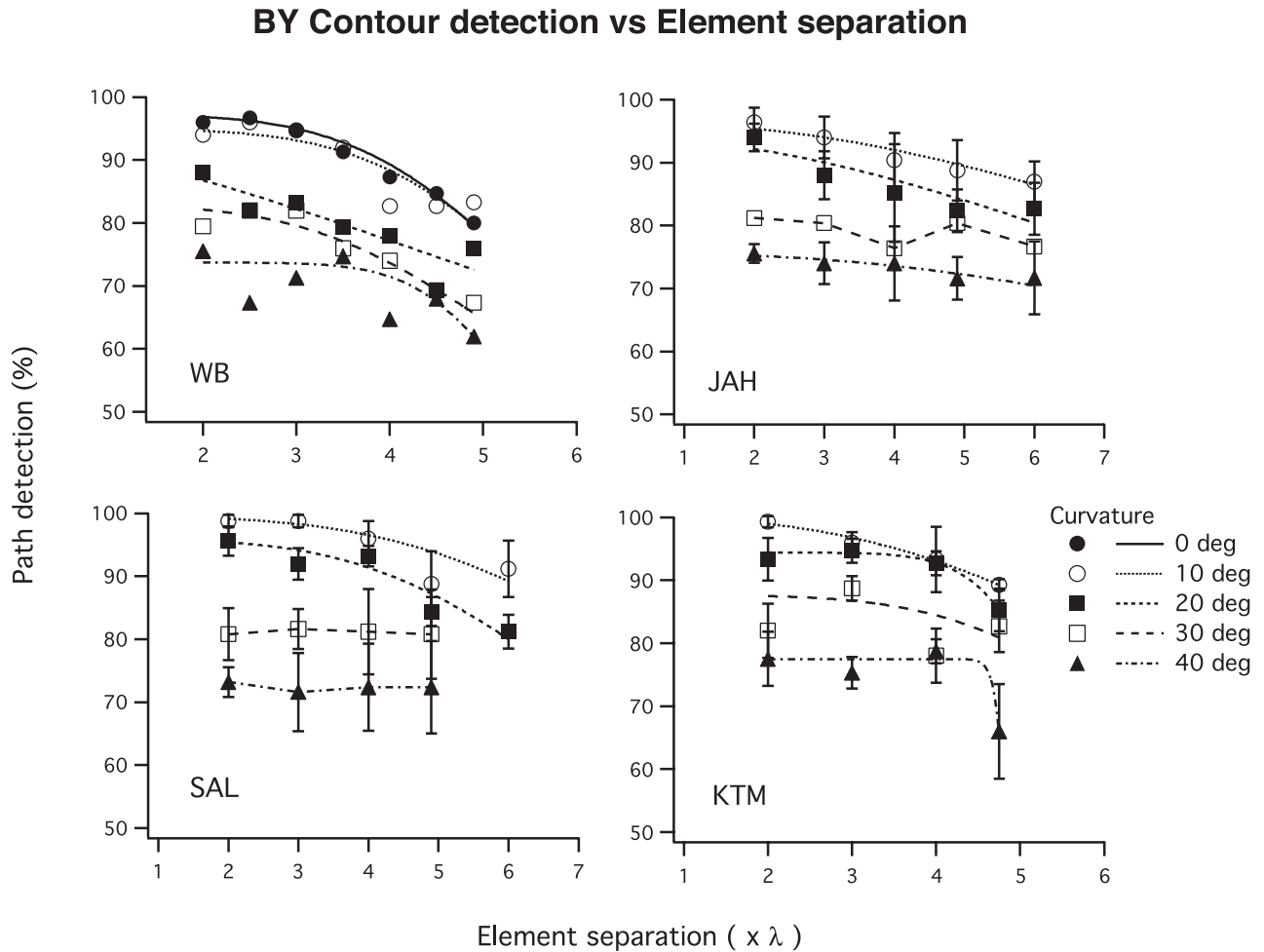


Fig. 5. Performance in jagged contour detection for all four subjects as a function of element separation at different curvatures for the BY mechanism. Smooth lines represent fits by eqn. (2). Note that three data sets could not be fitted. Error bars denote standard deviations.

Discussion

We investigated the effect of element spacing on contour integration to reveal the extent of long-range interactions involved in orientation linking and to provide more insight into the differential neural processes for the Ach, RG, and BY postreceptoral mechanisms. We found a differential dependence of contour integration on element separation for these three mechanisms; performance for the chromatic mechanisms, at all curvatures, declines more steeply with the increase in element separation than the Ach mechanism does. This suggests that contour integration by the chromatic mechanisms relies more on short-range interactions in comparison to the Ach mechanism, which may be limited by the spatial extent of V1 intrinsic connectivity. Contour integration for the RG mechanism declines at a smaller element separation than for the BY mechanism. However, as discussed later, contrast sensitivity may limit the spatial extent over which orientation linking is performed for RG stimuli. We also found that curvature and element separation do not interact; the detection of straight contours declines at the same element separations as detection of curved contours, suggesting that the length of the long-range

horizontal connections underlying the lateral interactions in V1 may be the main limiting factor. Moreover, the linear decrease of the critical separation with spatial frequency demonstrates that contour integration exhibits scale invariance for size and distance suggesting that smaller receptive fields have shorter connections than larger ones. Finally, we found no difference in critical element separation between open and closed contours for the three postreceptoral mechanisms and for a range of spatial frequencies.

In short, our data demonstrate that contour integration is spatially limited to no more than a few degrees in terms of element separation (up to 4.6 deg for Ach), with some deficit for the chromatic mechanisms compared to the Ach mechanism, and that this maximum distance for orientation linking is directly proportional to element size. Several fundamental questions arise from these findings. First, does the length of long-range connections in human V1 limit the spatial extent of contour integration? Second, is the length of the lateral interactions responsible for contour integration shorter for chromatic signals than for Ach signals? Third, does the length of the long-range connections depend on spatial frequency, as suggested by the size dependence of the critical separation?

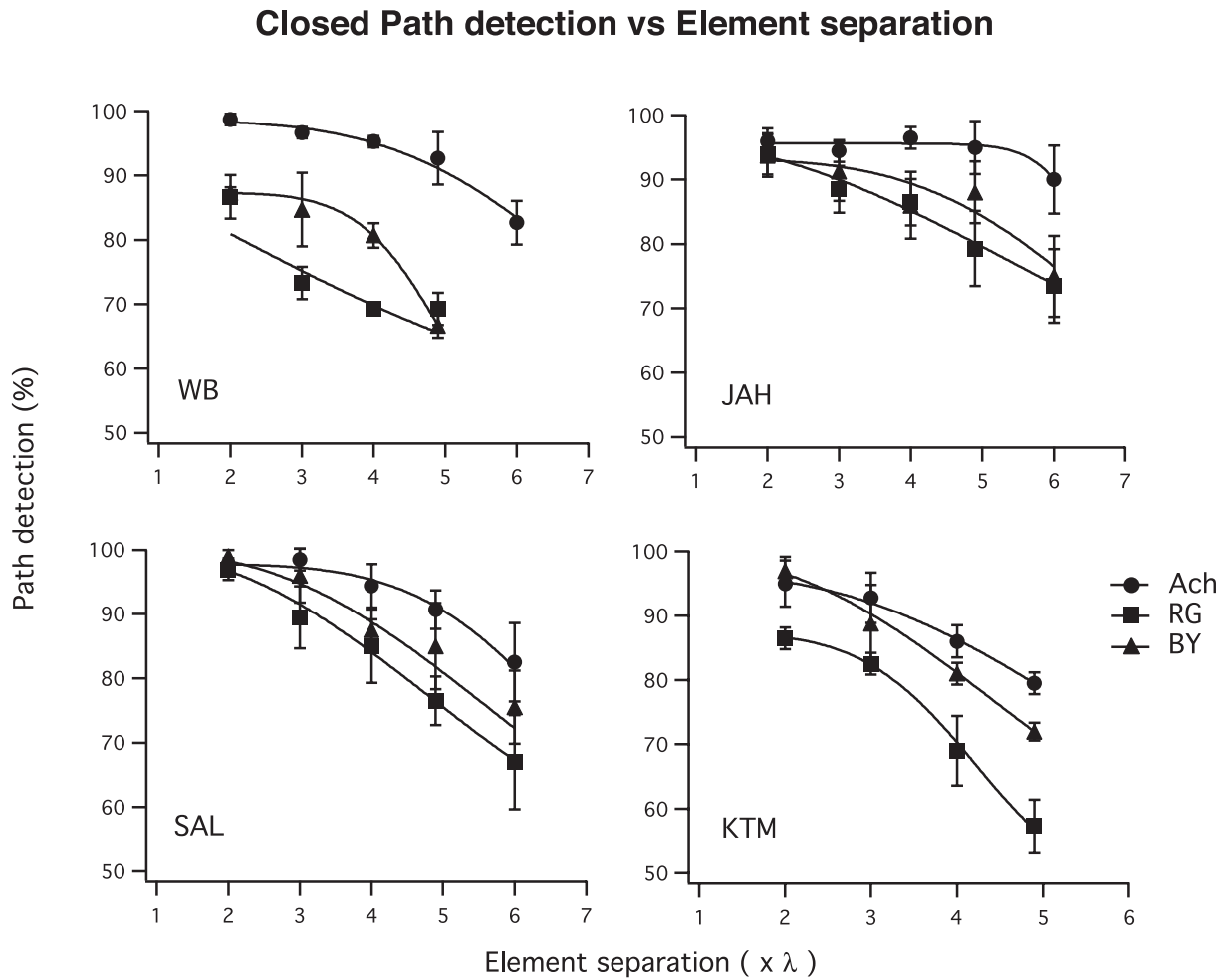


Fig. 6. Performance in closed contour detection for all four subjects as a function of element separation and for the three postreceptoral mechanisms (Ach, RG, & BY). Circles, squares, and triangles represent contour detection for achromatic, red–green, and blue–yellow stimuli, respectively. Smooth lines represent fits by eqn. (2). Error bars denote standard deviations.

Contour integration through long-range horizontal connections in V1?

Anatomical and physiological studies have suggested that the visual processing of spatially extended contours is mediated by long-range horizontal connections which promote the intracortical facilitation among co-oriented, co-axially cells in layer 2/3 of the striate cortex (Mitchison & Crick, 1982; Nelson & Frost, 1985; Ts'o et al., 1986; Gilbert & Wiesel, 1989; Malach et al., 1993; Kapadia et al., 1995; Bosking et al., 1997; Schmidt et al., 1997; Crook et al., 2002). Psychophysical and computational studies (Sha'ashua & Ullman, 1988; Parent & Zucker, 1989; Kellman & Shipley, 1991; Field et al., 1993; Kovacs, 1996; Yen & Finkel, 1998; Polat, 1999; Sigman et al., 2001; Geisler et al., 2001) have developed the Gestalt notion of "good continuation" (Kofka, 1935; Wertheimer, 1938) into rigorous accounts of contour grouping, which seem to parallel the functional nature of the long-range interactions in area V1. Moreover, a recent fMRI study of human visual cortex (Barnes et al., forthcoming) has found that area V1 shows an increased BOLD (blood oxygen level dependent) activity for contours made only of co-aligned and co-oriented elements, and not for contrast-defined or orientation-contrast-defined con-

tours, thus indicating that contour integration represents a special case of figure-ground cortical processing in human V1. Combined with the evidence that processing of illusory contours and figure-ground segregation occurs as early as area V1 (Lamme et al., 1992; Grosf et al., 1993; Lamme, 1995; Ramsden et al., 2001), it is very likely that this area plays a major role in contour integration. If the long-range horizontal connections between oriented V1 cells constitute the neural substrate for orientation linking, one may expect that they reflect some critical constraints on spatial integration performed in area V1.

On one hand, our results are consistent with the contrast-dependent long-range facilitation reported by Polat and Sagi (1993) and Polat and Norcia (1996); we find contour integration for the Ach mechanism is best at two wavelengths and drops significantly above 4–12 wavelengths depending on the spatial frequency of the elements. (Note that we did not test element separations at <2 wavelengths). Polat and Norcia (1996) reported visual evoked potential (VEP) data showing that contrast facilitation for collinear Gabor elements (3 cpd) increases for a target-to-mask distance below 3–4 deg, corresponding to 9–12 lambda. This is in very good agreement with the critical element separation we found at the same spatial frequency (about 3 deg, i.e. 10 lambda, see Fig. 6).

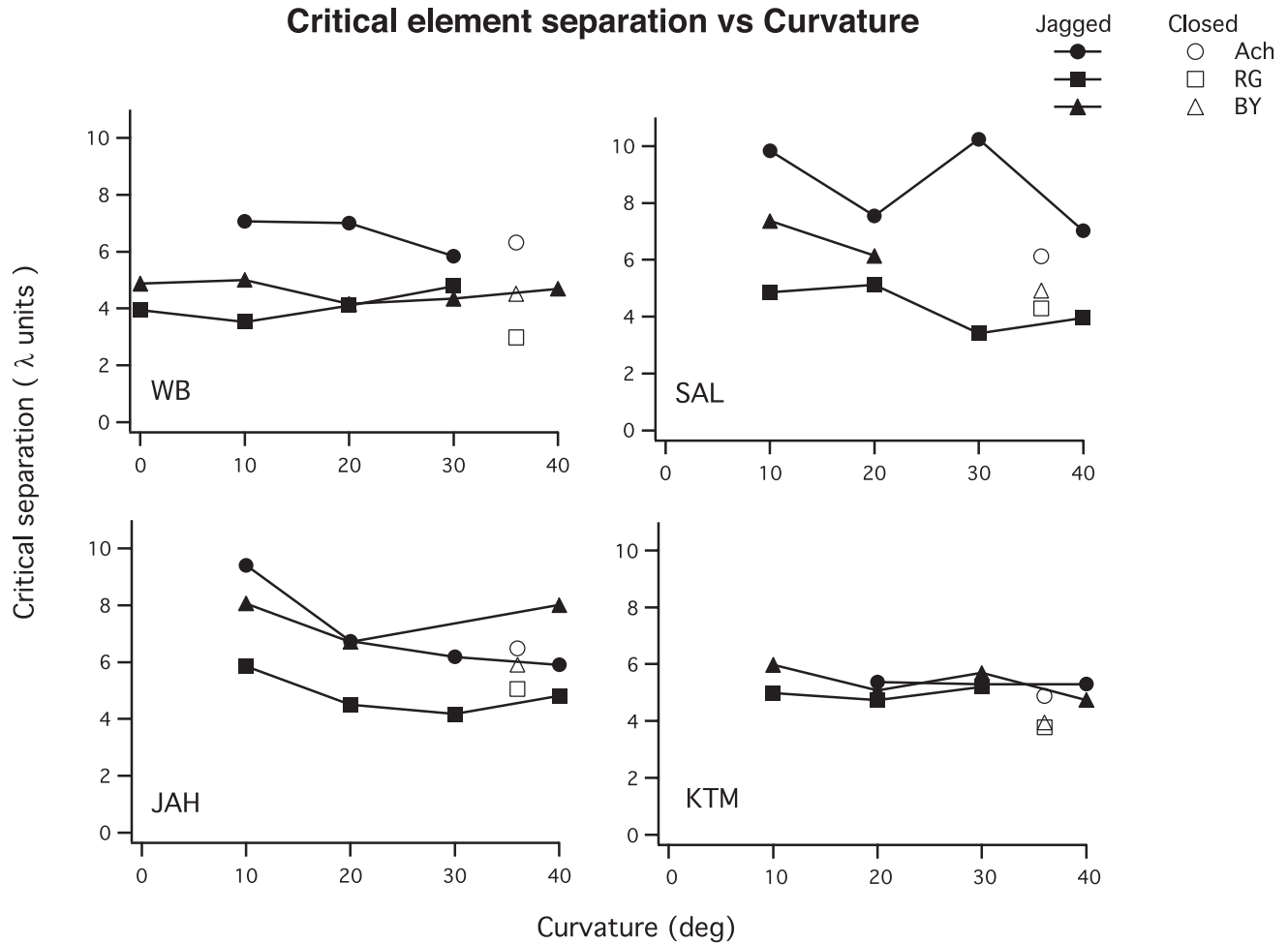


Fig. 7. Critical element separation as a function of curvature for all four subjects. Circles, squares, and triangles represent critical element separations for achromatic, red–green, and blue–yellow stimuli, respectively. Plain and open symbols represent critical element separations for detection of jagged contours and closed contours, respectively.

Combined with the fact that contrast facilitation like contour integration is maximal for co-aligned and co-oriented Gabor elements (Polat & Sagi, 1994; Polat & Norcia, 1996) suggests that long-range contrast facilitation and contour integration may rely on the same anatomical substrate.

On the other hand, Braun (1999) has recently claimed that the spatial range of the intrinsic connectivity of the striate cortex is greater than the limit of contour salience, and so unlikely to limit it. He reported that contours remain salient up to 9λ for 7 cpd elements, that is only 1.3 deg of visual angle, representing not more than 2 mm cortex at the relevant eccentricities. His claim was based on the assumption of intrinsic connectivity in striate cortex spanning distances up to 5–8 mm, much larger than his estimated critical spacing. However, these anatomical data are for cat and not primate striate cortex (Ts'o et al., 1986; Gilbert & Wiesel, 1989). Intrinsic connections in primate species have a more limited extent, about 1.5–2.0 mm (Rockland & Lund, 1983; Kenan-Vaknin et al., 1992; Amir et al., 1993; Sincich & Blasdel, 2001). Data on cortical magnification in human visual cortex (Cowey & Rolls, 1974; Slotnick et al., 2001) indicate that the critical separation of 4–5 deg we found for the Ach mechanism (at low spatial frequency) corresponds to a cortical distance of at least than 5 mm at

the most eccentric location of our stimuli. Consequently, due to the extreme cortical magnification of the human fovea, the critical separation in the central visual field may reach a few centimeters when expressed in cortical distance (Serenio et al., 1995). In this case, it is unlikely that the extent alone of the long-range horizontal connections limits contour integration. However, the spatial limitation we reported may still be carried by signal propagation through polysynaptic relays along the long-range horizontal connections or feedback from extrastriate areas, as suggested by Sincich and Blasdel (2001).

Color contour integration

Our results suggest that the lateral interactions responsible for contour integration are longer range for the Ach signal and shorter range for the chromatic signals. While there is evidence that the spatial extent of long-range connections in V1 is limiting contour integration for the Ach system, it is presently unclear what is limiting the chromatic mechanisms. No study has quantified the chromatic specificity of long-range horizontal connections in primate V1. However, some color-specific interactions between cytochrome-oxidase (CO) blob regions have been reported by Ts'o

Critical element separation & curvature

(averaged across subjects)

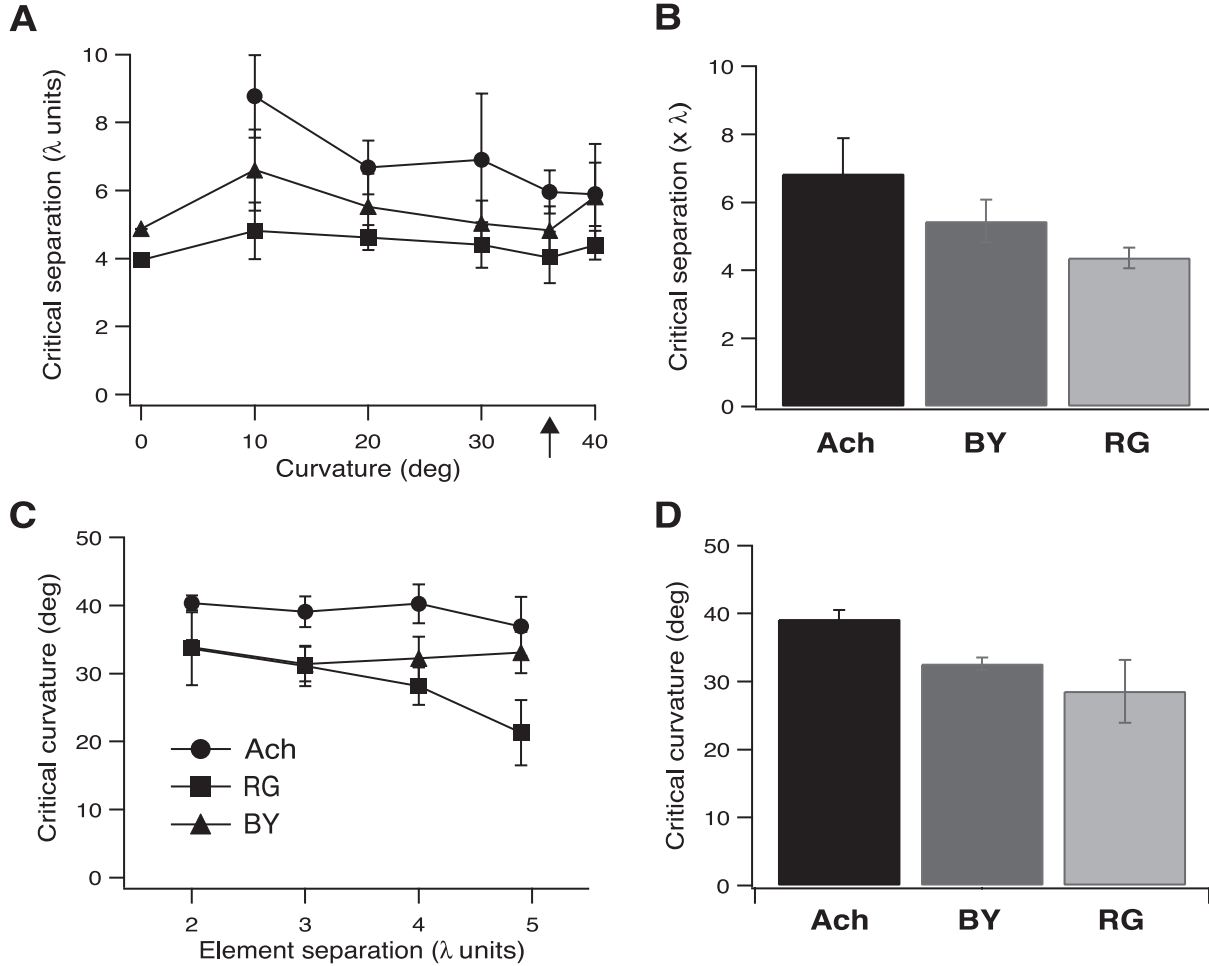


Fig. 8. A: Critical element separation averaged across the four subjects as a function of curvature (the arrow indicates the curvature of 36 deg corresponding to the closed contour condition). B: Critical element separation averaged across curvatures (closed contour included). C: Critical curvature averaged across the four subjects as a function of element separation. D: Critical curvature averaged across element separations. In A & C, circles, squares, and triangles represent achromatic, red–green, and blue–yellow stimuli, respectively. Error bars denote standard deviations.

and Gilbert (1988). More recently, Yoshioka et al. (1996) have examined the relationship of the patterns of intrinsic connections to CO blobs, interblobs, and ocular dominance bands in the superficial layers of macaque V1, and reported that interactions are found between functionally different regions. Roe and Ts'o (1999) have specifically looked at color connectivity between primate V1 and V2. They reported that interactions between nonoriented V1 and oriented V2 color cells exhibit a strong dependency on receptive-field overlap, suggesting a separate pathway for processing of color contour information (Livingstone & Hubel, 1984; Ts'o & Gilbert, 1988). Since area V2 also comprises intrinsic horizontal connections (Levitt et al., 1994; Malach et al., 1994) and feeds back to area V1 (Burkhalter, 1993; Bullier et al., 1996; Budd, 1998), it is possible that it plays a major role in color contour integration. Our finding that critical separations are significantly shorter for chromatic stimuli may indicate that horizontal connections are color selective. However, there is yet no

evidence that chromatic contour integration is subserved by short-range horizontal connections in V1, and other factors may play a role in limiting the critical separation for chromatic stimuli.

The steep decrease in RG contrast sensitivity with eccentricity (Mullen, 1991; Mullen & Kingdom, 1996) may have limited contour integration by the RG mechanism to the central visual field, thus explaining the lower critical separation we obtained for RG contours. Measuring contrast threshold elevations for contour detection as a function of contour eccentricity, we previously reported that above 2 deg of eccentricity, the RG mechanism already shows a significant deficit for integrating contours, while both the Ach and BY mechanisms are much less affected by contrast (Fig. 7 in Mullen et al., 2000; Mullen & Kingdom, 2002). Thus, it is likely that the steep decrease of RG contrast sensitivity with eccentricity is limiting its efficiency in contour integration at higher element separations. This is consistent with the lower critical separation of 2.9 ± 0.2 deg we found for the RG mecha-

Critical separation as a function of spatial frequency

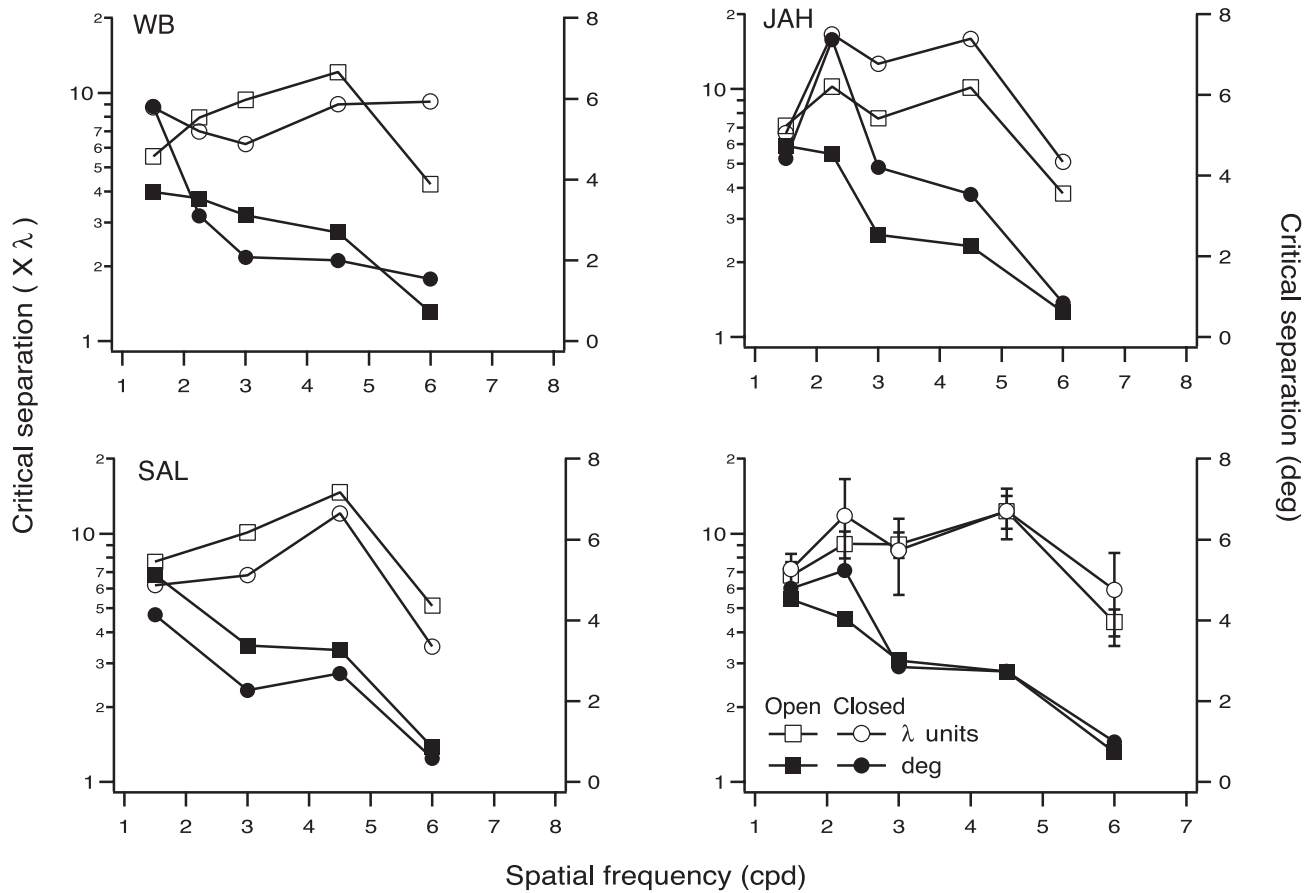


Fig. 9. Critical element separation as a function of spatial frequency for each subject and averaged across subjects (bottom right). In each graph, critical separations are expressed as multiples of the element wavelength (open symbols, left axis) and degrees of visual field (filled symbols, right axis). In both representations, circles and squares indicate closed and open contours, respectively. Error bars denote standard deviations.

nism. Mullen and Kingdom (2002) have recently reported that BY contrast sensitivity has a much shallower decline with eccentricity, comparable to that found for Ach stimuli up to 25 deg of eccentricity. Hence the loss of performance with increased element separation cannot be explained by a decrease of contrast sensitivity with eccentricity for the BY mechanism.

Moreover, according to Hess and Dakin (1997) (Fig. 3C, p. 603), one would expect to find a drop in critical curvature as a function of element separation if the peripheral elements were limiting contour integration. Fig. 8C shows that the critical curvature as a function of element separation is constant for both BY and Ach mechanisms, and decreases for the RG mechanism strengthening the fact that only the RG mechanism is affected by the visibility of the peripheral elements. In addition, our contour stimuli were constrained to pass through the central visual field in order to reduce the influence of eccentricity on element visibility (see Methods).

In a previous experiment investigating the perception of density *per se* in arrays of Gabor elements, we found that stimuli of identical physical densities are not perceived equally between postreceptoral mechanisms; there is a consistent bias in favor of

BY stimuli which are perceived as significantly more dense than Ach and RG stimuli (Beaudot & Mullen, 2000). We were able to fit these data to an occupancy model proposed by Allik and Tuulmets (1991) that accounts for the perception of numerosity in stimuli composed of dots. This occupancy model relies on the idea that each element of the stimulus has a neural occupancy much larger than the physical size of the element itself, and that it is the total neural occupancy that defines the perceived density and not the number of elements. By fitting our density data with this model, we estimated an occupancy radius for each mechanism (see Table 1), and we found that BY stimuli have a greater “occupancy” than RG or Ach stimuli. Thus, BY elements appear more dense because they “fill” more neural space. It is worth noting that this effect was also accompanied by a perceptual melting of the BY elements, in which the elements appear ill-defined and “melt” into the background. We hypothesized that the larger occupancy radius, perceptual melting effect, and density bias of the BY signal point to spatial processing differences among the postreceptoral mechanisms, which may include differences in their spatial filters, the sparseness of their spatial sampling, and differences in intracortical connectivity (Curcio et al., 1991; Dacey & Lee, 1994; Calkins

Table 1. Relation between occupancy diameter and critical spacing^a

| Mechanisms | Occupancy diameter (deg) | Critical spacing (deg) | Spacing-to-occupancy ratio |
|------------|--------------------------|------------------------|----------------------------|
| Ach | 1.35 | 4.6 | 3.41 |
| RG | 1.78 | 2.9 | 1.63 |
| BY | 2.44 | 3.6 | 1.48 |

^aThis table presents the occupancy diameter for each mechanism estimated from a previous study (Beaudot & Mullen, 2000) that investigated the perception of density, the critical separation for contour integration reported in the present study, and their ratio.

et al., 1998). When comparing with the present experiment, it is also noteworthy that the critical separation for contour integration is about 3.5 times the occupancy diameter for the Ach mechanism, and only 1.5 times for the BY mechanism (Table 1). The fact that contour integration by the BY mechanism relies more on short-range interactions than on long-range interactions suggests that it may be limited by its neural occupancy, or that these two phenomena result from a common limitation in the BY system. There are some evidence that the BY system is a part of the third geniculocortical pathway in primates (konio-cellular) which provides sparse inputs to the visual cortex, particularly in CO blobs of layer 3 (Martin et al., 1997; Ding & Casagrande, 1997). Interestingly, Yabuta and Callaway (1998) reported that 25% of pyramidal neurons in layer 2/3, that share a specific relationship with the CO blobs, have short axons and lack the distinct clusters of neurons with long-range horizontal axons. Such cells may carry out the chromatic short-range interactions for contour integration. However, the relationships between color processing, orientation selectivity, CO blobs, and the konio-cellular pathway are too fragmentary to support this prediction (Hendry & Reid, 2000; Landisman & Ts'o, 2002a,b).

Co-circular rule and scale invariance

Recent evidence from the investigation of the statistics of edge co-occurrences in natural scenes (Sigman et al., 2001; Geisler et al., 2001) have demonstrated the importance of the co-circular rule invented by Parent and Zucker (1989) and used to model the long-range horizontal intercolumnar interactions (Zucker et al., 1989; Yen & Finkel, 1998). Co-circularity is a natural extension of collinearity to the plane, and two edges are co-circular when they are tangent to the same circle (Fig. 10A). This co-circular rule is qualitatively similar to the “association field” proposed psychophysically by Field et al. (1993) as a particular implementation of the Gestalt principle of good continuation (Kofka, 1935; Wertheimer, 1938) applied to contour integration. One of the important geometrical properties of this simple co-circular rule is its scale invariance, that is orientation differences remain constant with distance scaling. Fig. 10A illustrates this relationship between scale invariance and the co-circularity rule. The three circles represent co-circular lines to the reference vertical edge segment they are tangent to. The two outer circles are scaled versions of the inner one, and the straight lines represent some scaling directions. One can see that the edge segments tangent to the circles intersected by each of these lines have a constant orientation. This can

Scale invariance and co-circular rule

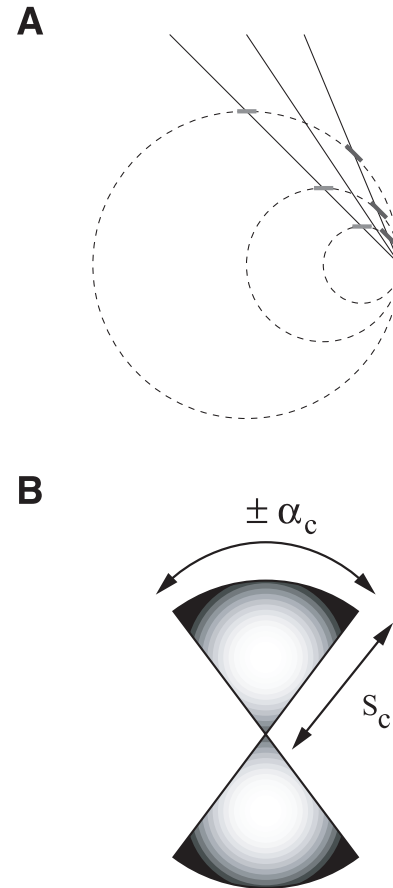


Fig. 10. A: Illustration of the relationship between co-circularity and scale invariance (see text for details). B: ‘Association field’ defined as the product of two separable functions.

be interpreted in the following way: increasing the separation between two edge segments does not affect their co-circular relationship. This property predicts that if contour integration follows the co-circular rule, then the critical curvature should not depend on the element separation.

Our first experiment demonstrates that it is precisely the case. We found that curvature does not affect the critical separation, and *vice-versa*, that element separation does not affect critical curvature, thus suggesting no interaction between these two dimensions. The fact that curvature and element separation do not interact supports both scale invariance and the co-circular rule in contour integration. This also suggests another way to look at the “association field” proposed by Field et al. (1993). This local grouping function can now be described as the product of two separable low-pass functions, one depending on distance and one depending on orientation contrast (Fig. 10B), and our data allow to specify each of these functions for the three postreceptoral mechanisms (α_c as the critical curvature, and S_c as the critical separation).

Open vs. closed contours

The fact that we found no difference in critical element separation between open and closed contours contradicts previous experimen-

tal results (Kovacs & Julesz, 1993; Pettet et al., 1998). In particular, Kovacs and Julesz (1993) reported that the critical separation for closed contours is about two times larger than for open contours (for elements of relatively high spatial frequency, 8.3 cpd). However, in these previous experiments the relative density between contour and background elements was changed across conditions, with either the spacing between contour elements varied and the spacing between background elements fixed (Kovacs & Julesz, 1993), or the spacing between contour elements fixed and the number of background elements varied (Pettet et al., 1998). The combination of the local density cue present in their stimuli and contour closure could thus explain the facilitation reported for the detection of closed contours.

This local density cue was absent in our stimuli, since spacing was the same between all elements (background and contour), and we found no differences in critical separation, suggesting that closure *per se* is not a peculiarity in contour integration. As we pointed out, however, asymptotic performances for closed contours (i.e. at 2λ) are always better than the ones for open contours of similar curvature. Closed contours are smooth, that is with a uniform direction of curvature, while our open contours are jagged, that is with the direction of curvature varying along the contour. The higher performance for closed contours is thus consistent with Pettet (1999) who demonstrated that smooth contours are more salient than jagged ones. As demonstrated in our two experiments, however, the effect of element spacing is the same for both types of contours, suggesting that their detection is limited by the same long-range mechanism.

Whether the long-range horizontal connections in V1 are sufficient for implementing the “association field” proposed by Field et al. (1993) is still controversial. Important questions remain, like whether V1 processing alone accounts for the global nature of contour integration, and what role the feedback from higher areas plays in shaping V1 activity related to global properties of visual stimuli (Lee et al., 1998; Bullier et al., 2001). To address psychophysically the relative contribution of feedforward, horizontal, and feedback processing, one may have to take the effect of element spacing into account in the investigation of the dynamics of contour integration (Hess et al., 2001; Beaudot, et al., 2002).

Acknowledgments

This study was funded by a CIHR grant to K.T. Mullen (MOP-10819). The authors also thank Jessica A. Haber for help in collecting data.

References

- ALLIK, J. & TUULMETS, T. (1991). Occupancy model of perceived numerosity. *Perception & Psychophysics* **49**(4), 303–314.
- AMIR, Y., HAREL, M. & MALACH, R. (1993). Cortical hierarchy reflected in the organization of intrinsic connections in macaque monkey visual cortex. *Journal of Comparative Neurology* **334**(1), 19–46.
- BARNES, G.R., DUMOULIN, S.O., ACHTMAN, R.A., BEAUDOT, W.H.A. & HESS, R.F. (forthcoming). Does contour integration represent a special case of figure-ground cortical processing? *Visual Neuroscience*.
- BEAUDOT, W.H.A. & MULLEN, K.T. (2000). Role of chromaticity, contrast, and local orientation cues in the perception of density. *Perception* **29**(5), 581–600.
- BEAUDOT, W.H.A., HESS, R.F. & MULLEN, K.T. (2002). Psychophysical evidence of cortical dynamics in contour integration. *Perception* **31** Suppl. (Abstract), p. 153.
- BOSKING, W.H., ZHANG, Y., SCHOFIELD, B. & FITZPATRICK, D. (1997). Orientation selectivity and the arrangement of horizontal connections in tree shrew striate cortex. *Journal of Neuroscience* **17**(6), 2112–2127.
- BRAUN, J. (1999). On the detection of salient contours. *Spatial Vision* **12**, 187–210.
- BUDD, J.M. (1998). Extrastriate feedback to primary visual cortex in primates: A quantitative analysis of connectivity. *Proceedings of the Royal Society B (London)* **265**(1400), 1037–1044.
- BULLIER, J., HUPE, J.M., JAMES, A. & GIRARD, P. (1996). Functional interactions between areas V1 and V2 in the monkey. *Journal of Physiology (Paris)* **90**(3–4), 217–220.
- BULLIER, J., HUPE, J.M., JAMES, A.C. & GIRARD, P. (2001). The role of feedback connections in shaping the responses of visual cortical neurons. *Progress in Brain Research* **134**, 193–204.
- BURKHALTER, A. (1993). Development of forward and feedback connections between areas V1 and V2 of human visual cortex. *Cerebral Cortex* **3**(5), 476–487.
- CALKINS, D.J., TSUKAMOTO, Y. & STERLING, P. (1998). Microcircuitry and mosaic of a blue–yellow ganglion cell in the primate retina. *Journal of Neuroscience* **18**(9), 3373–3385.
- COLE, G.R. & HINE, T. (1992). Computation of cone contrasts for color vision research. *Behavioural Research, Methods and Instrumentation* **24**, 22–27.
- COWEY, A. & ROLLS, E.T. (1974). Human cortical magnification factor and its relation to visual acuity. *Experimental Brain Research* **21**(5), 447–454.
- CROOK, J.M., ENGELMANN, R. & LOWEL, S. (2002). GABA-inactivation attenuates colinear facilitation in cat primary visual cortex. *Experimental Brain Research* **143**(3), 295–302.
- CURCIO, C.A., ALLEN, K.A., SLOAN, K.L., LEREA, C.L., HURLEY, J.B., KLOCK, I.B. & MILAM, A.H. (1991). Distribution and morphology of human cone photoreceptors stained with anti-blue opsin. *Journal of Comparative Neurology* **312**, 610–624.
- DACEY, D.M. & LEE, B.B. (1994). The ‘blue-on’ opponent pathway in primate retina originates from a distinct bistratified ganglion cell type. *Nature* **367**(6465), 731–735.
- DING, Y. & CASAGRANDE, V.A. (1997). The distribution and morphology of LGN K pathway axons within the layers and CO blobs of owl monkey V1. *Visual Neuroscience* **14**(4), 691–704.
- ELDER, J. & ZUCKER, S. (1993). The effect of contour closure on the rapid discrimination of two-dimensional shapes. *Vision Research* **33**, 981–991.
- FIELD, D.J., HAYES, A. & HESS, R.F. (1993). Contour integration by the human visual system: Evidence for a local ‘association field’. *Vision Research* **33**, 173–193.
- GEISLER, W.S., PERRY, J.S., SUPER, B.J. & GALLOGLY, D.P. (2001). Edge co-occurrence in natural images predicts contour grouping performance. *Vision Research* **41**(6), 711–724.
- GILBERT, C.D. & WIESEL, T.N. (1989). Columnar specificity of intrinsic horizontal and corticocortical connections in cat visual cortex. *Journal of Neuroscience* **9**(7), 2432–2442.
- GROSOFF, D.H., SHAPLEY, R.M. & HAWKEN, M.J. (1993). Macaque V1 neurons can signal ‘illusory’ contours. *Nature* **365**(6446), 550–552.
- HENDRY, S.H. & REID, R.C. (2000). The koniocellular pathway in primate vision. *Annual Review of Neuroscience* **23**, 127–153.
- HESS, R.F. & DAKIN, S.C. (1997). Absence of contour linking in peripheral vision. *Nature* **390**(6660), 602–604.
- HESS, R. & FIELD, D. (1999). Integration of contours: New insights. *Trends in Cognitive Science* **3**(12), 480–486.
- HESS, R.F., BEAUDOT, W.H.A. & MULLEN, K.T. (2001). Dynamics of contour integration. *Vision Research* **41**(8), 1023–1037.
- KAPADIA, M.K., ITO, M., GILBERT, C.D. & WESTHEIMER, G. (1995). Improvement in visual sensitivity by changes in local context: Parallel studies in human observers and in V1 of alert monkeys. *Neuron* **15**(4), 843–856.
- KELLMAN, P.J. & SHIPLEY, T.F. (1991). A theory of visual interpolation in object perception. *Cognitive Psychology* **23**, 141–221.
- KENAN-VAKNIN, G., OUAKNINE, G.E., RAZON, N. & MALACH, R. (1992). Organization of layers II–III connections in human visual cortex revealed by *in vitro* injections of biocytin. *Brain Research* **594**(2), 339–342.
- KOFFKA, K. (1935). *Principles of Gestalt Psychology*. New York: Harcourt & Brace.
- KOVACS, I. (1996). Gestalten of today: Early processing of visual contours and surfaces. *Behavioral Brain Research* **82**(1), 1–11.
- KOVÁCS, I. & JULESZ, B. (1993). A closed curve is much more than an incomplete one: Effect of closure in figure-ground segmentation. *Proceedings of the National Academy of Sciences of the U.S.A.* **90**, 7495–7497.
- KOVACS, I., KOZMA, P., FEHER, A. & BENEDEK, G. (1999). Late maturation

- of visual spatial integration in humans. *Proceedings of the National Academy of Sciences of the U.S.A.* **96**(21), 12204–12209.
- KUBOVY, M., HOLCOMBE, A.O. & WAGEMANS, J. (1998). On the lawfulness of grouping by proximity. *Cognitive Psychology* **35**, 71–98.
- LAMME, V.A. (1995). The neurophysiology of figure-ground segregation in primary visual cortex. *Journal of Neuroscience* **15**(2), 1605–1615.
- LAMME, V.A., VAN DIJK, B.W. & SPEKREIJSE, H. (1992). Texture segregation is processed by primary visual cortex in man and monkey. Evidence from VEP experiments. *Vision Research* **32**(5), 797–807.
- LANDISMAN, C.E. & TS'O, D.Y. (2002a). Color processing in macaque striate cortex: Relationships to ocular dominance, cytochrome oxidase, and orientation. *Journal of Neurophysiology* **87**(6), 3126–3137.
- LANDISMAN, C.E. & TS'O, D.Y. (2002b). Color processing in macaque striate cortex: Electrophysiological properties. *Journal of Neurophysiology* **87**(6), 3138–3151.
- LEE, T.S., MUMFORD, D., ROMERO, R. & LAMME, V.A. (1998). The role of the primary visual cortex in higher level vision. *Vision Research* **38**(15–16), 2429–2454.
- LEVITT, J.B., YOSHIOKA, T. & LUND, J.S. (1994). Intrinsic cortical connections in macaque visual area V2: Evidence for interaction between different functional streams. *Journal of Comparative Neurology* **342**(4), 551–570.
- LIVINGSTONE, M.S. & HUBEL, D.H. (1984). Anatomy and physiology of a color system in the primate visual cortex. *Journal of Neuroscience* **4**(1), 309–356.
- MALACH, R., AMIR, Y., HAREL, M. & GRINVALD, A. (1993). Relationship between intrinsic connections and functional architecture revealed by optical imaging and *in vivo* targeted biocytin injections in primate striate cortex. *Proceedings of the National Academy of Sciences of the U.S.A.* **90**(22), 10469–10473.
- MALACH, R., TOOTELL, R.B. & MALONEK, D. (1994). Relationship between orientation domains, cytochrome oxidase stripes, and intrinsic horizontal connections in squirrel monkey area V2. *Cerebral Cortex* **4**(2), 151–165.
- MARTIN, P.R., WHITE, A.J., GOODCHILD, A.K., WILDER, H.D. & SEFTON, A.E. (1997). Evidence that blue-on cells are part of the third geniculocortical pathway in primates. *European Journal of Neuroscience* **9**(7), 1536–1541.
- MCILHAGGA, W.H. & MULLEN, K.T. (1996). Contour integration with colour and luminance contrast. *Vision Research* **36**(9), 1265–1279.
- MITCHISON, G. & CRICK, F. (1982). Long axons within the striate cortex: their distribution, orientation, and patterns of connection. *Proceedings of the National Academy of Sciences of the U.S.A.* **79**(11), 3661–3665.
- MULLEN, K.T. (1991). Colour vision as a postreceptoral specialization of the central visual field. *Vision Research* **31**, 119–130.
- MULLEN, K.T. & KINGDOM, F.A. (1996). Losses in peripheral colour sensitivity predicted from “hit and miss” post-receptoral cone connections. *Vision Research* **36**(13), 1995–2000.
- MULLEN, K.T. & KINGDOM, F.A. (2002). Differential distributions of red–green and blue–yellow cone opponency across the visual field. *Visual Neuroscience* **19**(1), 109–118.
- MULLEN, K.T., BEAUDOT, W.H.A. & MCILHAGGA, W.H. (2000). Contour integration in color vision: a common process for the blue–yellow, red–green and luminance mechanisms? *Vision Research* **40**(6), 639–655.
- NELSON, J.I. & FROST, B.J. (1985). Intracortical facilitation among co-oriented, co-axially aligned simple cells in cat striate cortex. *Experimental Brain Research* **61**(1), 54–61.
- PARENT, P. & ZUCKER, S. (1989). Trace inference, curvature consistency and curve detection. *IEEE Transactions on Pattern Analysis and Machine Intelligence* **11**, 823–839.
- PENNEFATHER, P.M., CHANDNA, A., KOVACS, I., POLAT, U. & NORCIA, A.M. (1999). Contour detection threshold: repeatability and learning with ‘contour cards’. *Spatial Vision* **12**(3), 257–266.
- PETTET, M.W. (1999). Shape and contour detection. *Vision Research* **38**, 551–557.
- PETTET, M.W., MCKEE, S.P. & GRZYWACZ, N.M. (1998). Constraints on long-range interactions mediating contour detection. *Vision Research* **38**, 865–879.
- POLAT, U. (1999). Functional architecture of long-range perceptual interactions. *Spatial Vision* **12**(2), 143–162.
- POLAT, U. & SAGI, D. (1993). Lateral interactions between spatial channels: Suppression and facilitation revealed by lateral masking experiments. *Vision Research* **33**, 993–999.
- POLAT, U. & SAGI, D. (1994). The architecture of perceptual spatial interactions. *Vision Research* **34**(1), 73–78.
- POLAT, U. & NORCIA, A.M. (1996). Neurophysiological evidence for contrast dependent long-range facilitation and suppression in the human visual cortex. *Vision Research* **36**(14), 2099–2109.
- RAMSDEN, B.M., HUNG, C.P. & ROE, A.W. (2001). Real and illusory contour processing in area V1 of the primate: A cortical balancing act. *Cerebral Cortex* **11**(7), 648–665.
- ROCKLAND, K.S. & LUND, J.S. (1983). Intrinsic laminar lattice connections in primate visual cortex. *Journal of Comparative Neurology* **216**(3), 303–318.
- ROE, A.W. & TS'O, D.Y. (1999). Specificity of color connectivity between primate V1 and V2. *Journal of Neurophysiology* **82**(5), 2719–2730.
- ROVAMO, J.M., KANKAANPÄÄ, M.I. & HALLIKAINEN, J. (2001). Spatial neural modulation transfer function of human foveal visual system for equiluminous chromatic gratings. *Vision Research* **41**(13), 1659–1667.
- SCHMIDT, K.E., GOEBEL, R., LOWEL, S. & SINGER, W. (1997). The perceptual grouping criterion of colinearity is reflected by anisotropies of connections in the primary visual cortex. *European Journal of Neuroscience* **9**(5), 1083–1089.
- SERENO, M.I., DALE, A.M., REPPAS, J.B., KWONG, K.K., BELLIVEAU, J.W., BRADY, T.J., ROSEN, B.R. & TOOTELL, R.B.H. (1995). Borders of multiple visual areas in human revealed by functional magnetic resonance imaging. *Science* **268**, 889–893.
- SHA'ASHUA, A. & ULLMAN, S. (1988). Structural saliency: The detection of globally salient structures using a locally connected network. *Proceedings of the Second International Conference on Computer Vision*, pp. 321–327.
- SIGMAN, M., CECCHI, G.A., GILBERT, C.D. & MAGNASCO, M.O. (2001). On a common circle: Natural scenes and Gestalt rules. *Proceedings of the National Academy of Sciences of the U.S.A.* **98**(4), 1935–1940.
- SINCICH, L.C. & BLASDEL, G.G. (2001). Oriented axon projections in primary visual cortex of the monkey. *Journal of Neuroscience* **21**(12), 4416–4426.
- SLOTNICK, S.D., KLEIN, S.A., CARNEY, T. & SUTTER, E.E. (2001). Electrophysiological estimate of human cortical magnification. *Clinical Neurophysiology* **112**, 1349–1356.
- SMITH, V.C. & POKORNY, J. (1975). Spectral sensitivity of the foveal cone photopigments between 400 and 500 nm. *Vision Research* **15**, 161–171.
- TS'O, D.Y. & GILBERT, C.D. (1988). The organization of chromatic and spatial interactions in the primate striate cortex. *Journal of Neuroscience* **8**, 1712–1727.
- TS'O, D.Y., GILBERT, C.D. & WIESEL, T.N. (1986). Relationships between horizontal interactions and functional architecture in cat striate cortex as revealed by cross-correlation analysis. *Journal of Neuroscience* **6**(4), 1160–1170.
- UTTAL, W.R. (1987). *The Perception of Dotted Forms*. Hillsdale, New Jersey: Erlbaum.
- VASSILEV, A., ZLATKOVA, M. & MITOVA, L. (1989). Length and width summation in human vision at different background levels. *Experimental Brain Research* **74**(2), 421–426.
- WERTHEIMER, M. (1938). *Laws of Organization in Perceptual Forms*. London: Harcourt, Brace & Jovanovitch.
- YABUTA, N.H. & CALLAWAY, E.M. (1998). Cytochrome-oxidase blobs and intrinsic horizontal connections of layer 2/3 pyramidal neurons in primate V1. *Visual Neuroscience* **15**(6), 1007–1027.
- YEN, S.C. & FINKEL, L.H. (1998). Extraction of perceptually salient contours by striate cortical networks. *Vision Research* **38**, 719–741.
- YOSHIOKA, T., BLASDEL, G.G., LEVITT, J.B. & LUND, J.S. (1996). Relation between patterns of intrinsic lateral connectivity, ocular dominance, and cytochrome oxidase-reactive regions in macaque monkey striate cortex. *Cerebral Cortex* **6**(2), 297–310.
- ZIPSER, K., LAMME, V.A. & SCHILLER, P.H. (1996). Contextual modulation in primary visual cortex. *Journal of Neuroscience* **16**(22), 7376–7389.
- ZUCKER, S.W. & DAVIS, S. (1988). Points and endpoints: A size/spacing constraint for dot grouping. *Perception* **17**, 229–247.
- ZUCKER, S.W., DOBBINS, A. & IVERSON, L. (1989). Two stages of curve detection suggest two styles of visual computation. *Neural Computation* **1**(1), 68–81.